10380 *Biochemistry* **2009,** *48,* 10380–10388
DOI: 10.1021/bi901401e

BIOCHEMISTRY
including biophysical chemistry & molecular biology
Article

Role of Hydrophobic and Electrostatic Interactions in Coiled Coil Stability and Specificity[†]

Jody M. Mason,*[,‡,⊥] Urs B. Hagemann,[‡,@] and Katja M. Arndt*[,‡,§,∥]

[‡]*Institute of Biology III, Albert-Ludwigs University of Freiburg, Schaenzlestrasse 1, D-79104 Freiburg, Germany,* [§]*Center for Biological Signaling Studies (bioss), Albert-Ludwigs University of Freiburg, D-79104 Freiburg, Germany, and* [∥]*Freiburg Institute for Advanced Studies, School of Life Sciences (FRIAS-LIFENET), Albert-Ludwigs University of Freiburg, D-79104 Freiburg, Germany* [⊥]*Present address: Department of Biological Sciences, University of Essex, Wivenhoe Park, Colchester CO4 3SQ, U.K.* [@]*Present address: Affitech AS, Gaustadalleen 21, N-0349 Oslo, Norway.*

Received August 12, 2009; Revised Manuscript Received September 8, 2009

ABSTRACT: We have screened two coiled coil-forming libraries in which core **a** and electrostatic **e**/**g** positions have been partially randomized. We observed the relative ability of these residues to confer coiled coil stability using a protein-fragment complementation assay. Our studies continue with the Jun/Fos activator protein-1 (AP-1) leucine zipper complex, as it provides a valid therapeutic target, while representing one of the more simplistic examples of quaternary structure. In mammalian cells, 28 possible dimeric interactions result from combinations of cJun, JunB, JunD, cFos, FosB, Fra1, and Fra2. Consequently, peptides designed to target particular oncogenic members must bind with high affinity and also be specific if they are to function as desired. We have therefore tested the ability of core and electrostatic interactions to confer stable and specific peptides. A previously selected peptide (FosW) formed the template for the core and electrostatic libraries. The winner from the core randomization ($FosW_{Core}$) bound specifically to cJun relative to cFos, FosB, Fra1, Fra2, and the $FosW_{Core}$ homodimer, as verified by thermal melting analyses and growth competitions in the presence of either a negative control "mock" peptide or a competitor fusion peptide (cFos−FosB−Fra1−Fra2). In contrast, the winner from the electrostatic **e**/**g** randomization ($FosW_{e/g}$) bound to all respective complexes with high stability, suggesting that the more significant energetic contributions made by core residues may be enough to generate specificity as a consequence of positive design.

Understanding how one protein recognizes and binds another with high specificity is advantageous for mapping protein networks and in devising peptide and peptidomimetic antagonists that can mimic natural proteins. In doing so, peptide antagonists can bind and sequester proteins that are behaving abnormally and that consequently could give rise to a pathogenic phenotype.

Our studies focus on the Jun−Fos activator protein-1 (AP-1)[1] motif (*1*−*3*). This protein contains a repetitive and yet highly specific coiled coil motif that is responsible for mediating dimerization. AP-1 is an ideal test bed for our experimentation because (i) coiled coils represent a highly simplistic example of quaternary structure (*4*, *5*); (ii) coiled coils are distributed ubiquitously both intracellularly and extracellularly, mediating a wide range of important and highly specific interactions in motifs such as transcription factors (*6*), viral receptors (*7*, *8*), muscle contraction (*9*), cell signaling (*10*), molecular chaperones (*11*), and fertilization domains (*12*); and (iii) many coiled coils represent potential sites for therapeutic intervention. For example, the Jun−Fos system forms the heterodimeric transcription factor AP-1, and it is known that particular homologues are deregulated or overexpressed in tumorigenic phenotypes. AP-1 is thought to represent a legitimate target since it is found at the end of several cell signaling cascades (*2*). The ultimate aim is to sequester one half of AP-1 as a nonfunctional heterodimer using an orally available peptidomimetic. Achieving this goal first requires an understanding of the molecular mechanisms of specific protein−protein interactions. Indeed, while it is relatively straightforward to design in the positive (desired) direction, considerably less is known about how to do so in a highly specific manner. This is particularly important in forming specific protein−protein interactions, in which there are thousands of other potential proteins competing for an interaction, some of which can be very close in sequence, and therefore in structure. Using peptides as the starting point for drug design offers a number of advantages over conventional small molecule-based approaches (*13*, *14*). For example, peptides are less likely to be toxic than small molecule inhibitors since they are more natural and can be degraded over time. Peptides are also more likely to be able to inhibit protein−protein interactions in which the interface is large. They can be synthesized (or recombinantly expressed) both quickly and inexpensively to high purity (e.g., using Fmoc chemistry). In addition, they are generally stable, are easy to store, and often interact with important biologically relevant target sites. They can be readily modified to deal with protease susceptibility issues and optimized to meet the lipid−water partition coefficient (logP) required for membrane permeability (typically < 5).

[†]The work was funded by the Emmy-Noether Program of the German Research Foundation (DFG; Ar373/1-1 and 1-2), the José Carreras Leukemia Foundation (DJCLS R 06/12), and the Excellence Institute of the German Federal and State Governments (EXC 294).

*To whom correspondence should be addressed. Telephone: +49-761-203-2748 or -2763. Fax: +49-761-203-2745. E-mail: katja@biologie.uni-freiburg.de or jmason@essex.ac.uk.

[1]Abbreviations: DHFR, dihydrofolate reductase; PCA, protein-fragment complementation assay; AP-1, activator protein-1.

 Published on Web 09/10/2009

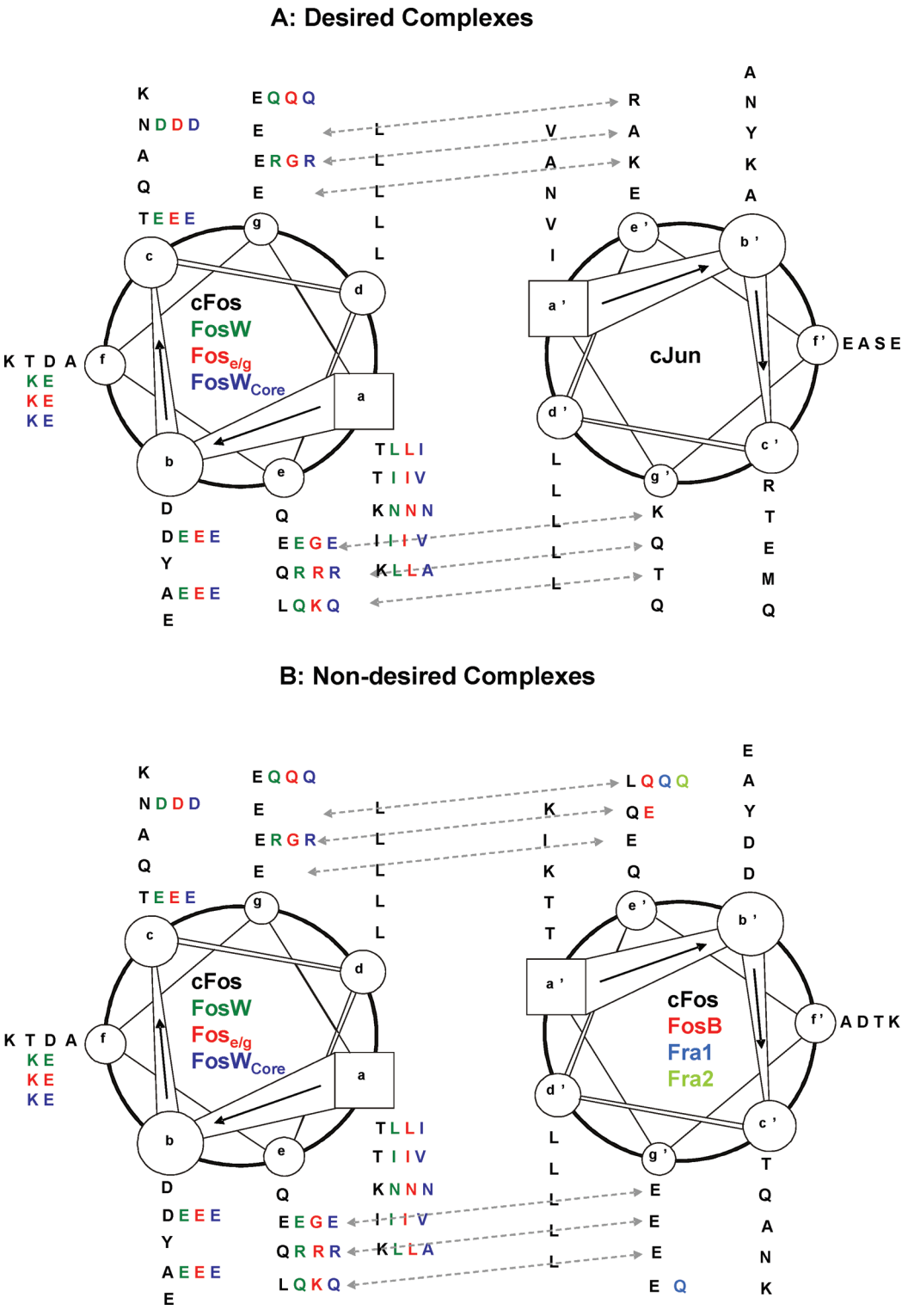

FIGURE 1: Helical wheel diagram highlighting the interaction pattern of cFos and three selected Fos variants with (A) cJun or (B) cFos, FosB, Fra1, and Fra2. Residues for cFos are colored black. Residues for FosW that differ from those of cFos are colored green. Residues for Fos $W_{e/g}$ that differ from those of cFos are colored red, and residues for $FosW_{Core}$ that differ from those of cFos are colored blue. Note that all **b**, **c**, and **f** positions for FosW, $FosW_{e/g}$, and $FosW_{Core}$ are identical. Also, the **a** residues of FosW and $FosW_{e/g}$ are identical, and the **e** and **g** residues of FosW and $FosW_{Core}$ are identical. This allows us to look at the contribution made to stability by selected core and **e**/**g** residues, respectively, relative to the FosW molecule.

To probe how specificity in protein−protein interactions is achieved, we have employed the use of a semirational library design approach. This was previously conducted in combination with a protein-fragment complementation assay (PCA) (*15*−*17*) to identify "winner" peptides (JunW and FosW) with high affinity for cFos and cJun, respectively. To extend our search criteria, we have performed PCA selections with libraries based on the FosW framework, a peptide based on the parallel and dimeric Jun/Fos coiled coil interaction that is known to bind to cJun (*17*, *18*). The libraries were semirandomized either at core **a** or at electrostatic **e**/**g** positions (Figure 1), and PCA selection was conducted to identify and enrich interacting helices. Thermal

denaturation experiments of isolated dimers have been used to establish the stability and specificity of core **a** or electrostatic **e**/**g** residue PCA winners for the cJun target peptide relative to a range of Fos-based homologues. This work, therefore, addresses the ability of PCA selected **a** and **e**/**g** residues to exert both stability and specificity on the Jun−Fos AP-1 system. Addressing this issue will further our understanding of factors leading to stable and specific protein−protein interactions.

Lastly, we have investigated whether specificity can be generated as a trade-off for desired-state stability, as previously suggested (*19*). We anticipate that this can be achieved provided that the energetic contribution to nondesired, otherwise energetically similar states is simultaneously destabilizing. If specificity is a trade-off for desired-state stability, then residue options and heptad positions able to confer the largest increase in desired-state stability are clearly the most favorable to introduce provided that the energetic contribution to nondesired, otherwise energetically similar states is simultaneously destabilizing.

MATERIALS AND METHODS

Library Design and Cloning. Library design and cloning have been described elsewhere (*17*). Briefly, megaprimers were synthesized, including relevant degenerate codons for library residue options, and a fill-in reaction was performed, resulting in 111 bp double-stranded oligonucleotides. These were cloned via NheI and AscI sites into a pQE16 derivative (Qiagen) containing a G/S linker tagged to fragment 1 [pAR230d; cJun; ampicillin resistance, Amp^R (*17*)] and fragment 2 [pAR300d; FosW library, chloramphenicol resistance, Cm^R (*17*)] of murine dihydrofolate reductase (mDHFR), respectively, resulting in pAR230d-cJun-DHFR1 and pAR300d-*FosW-library*-DHFR2. The Fos homologue fusion peptide competitor comprised cFos−FosB−Fra1−Fra2 fusion peptide (underlined), each separated by short linkers designed to include helix caps and discourage helix prolongation by including a Pro residue: ASTDTLQAETDQLEDEKYALQTEIANLLKEKEKLGAPVASTDRLQAETDQLEEEKYELESEIAELQKEKERLGAPASTDFLQAETDKLEDEKYGLQREIEELQKQKERLGAPASTEKLQAETEELEEEKYGLQKEIAELQKEKEKLGAP. The corresponding gene, which was purchased from epochbiolabs (Sugarland, TX), carried an NheI and AscI site (bold) for cloning into pAR410d (tetracyclin resistance, Tet^R) (*17*) and consequently lacked a DHFR fragment fusion: GG GCC **GCT AGC** ACG GAT ACC TTA CAA GCG GAG ACC GAC CAG CTG AA GAT GAG AAG TAC GCG CTG CAG ACT GAA ATT GCA AAC TTA CTG AG GAG AAA GAA AAA TTG GGT GCA CCG GTG GCC AGC ACC GAC CGT CTG CAG GCT GAA ACG GAT CAA TTA GAG GAA GAA AAA TAT GAA CTG GAG AGC GAAATCGC-GGAGCTGCAG AAA GAA AAG GAA CGC CTG GGG GCG CCA GCA AGT ACT GAT TTT CTG CAG GCC GAA ACC GAC AAA TTG GAG GAC GAA AAG TAT GGC CTG CAG CGT GAA ATC GAG GAA CTG CAA AAA CAG AAA GAA CGT CTG GGT GCC CCG GCG AGC ACC GAA AAA TTG CAG GCA GAG ACG GAA GAG CTG GAA GAG GAA AAA TAC GGT CTG CAG AAA GAA ATC GCT GAA CTG CAG AAG GAG AAA GAA AAA CTG **GGC GCG CCT** CCC GG.

In addition, an AgeI site (underlined) was introduced between cFos and FosB to allow future introduction of alternative competing helices between the NheI and AgeI sites. As a proof of the expression and structural integrity of this fusion helix, the construct was His-tagged at the N-terminus and fused via a Gly/Ser linker (SGSSGTSSGTS) to enhanced green fluorescent protein (eGFP) at the C-terminus, resulting in the pAR410d-cFos-FosB-Fra1-Fra2-eGFP plasmid. All proteins were under control of a lac promoter, and expression was induced with 1 mM isopropyl β-D-1-thiogalactopyranoside (IPTG). Elution from an Ni-NTA column gave a green protein that was consistent with the intact fusion helix. For PCA selection, library plasmids (Cm^R) were transformed into BL21 cells (Stratagene) containing the target plasmid (Amp^R) and pREP4 (Qiagen; expressing the lac repressor and conferring kanamycin resistance, Kan^R). To assay bacterial growth rates in the presence of the Fos homologues, the fourth competing fusion peptide plasmid was also transformed (Tet^R). To assess library quality, we sequenced pools and single clones and found approximately equal distributions of varied amino acids. Pooled colonies exceeded the library size 5−10-fold.

Selection of Winner Peptides. The protein-fragment complementation assay has been described in detail previously (*15*, *16*). Briefly, target and library peptides are tagged at the genetic level to either half of mDHFR (pAR230d-cJun-DHFR1 and pAR300d-*FosW-library*-DHFR2). Only two interacting helices will bring the two halves of the enzyme into the proximity of each other, render the enzyme active, and result in colony formation on M9 minimal medium plates with 1 μg/mL trimethoprim to inhibit bacterial DHFR [mammalian DHFR has a 12000-fold lower affinity for trimethoprim than bacterial DHFR (*20*)]. We have previously shown that PCA selected winners are dimeric (*24*, *25*) (U. B. Hagemann et al., unpublished data). Indeed, peptides adopting higher-order or multiple oligomeric states or displaying incorrect helix orientation are highly unlikely since the PCA system aligns peptides in a parallel orientation during selection and ensures that specific helices are both parallel and dimeric. A third competing peptide is expressed on a plasmid conferring tetracycline resistance but is not fused to a DHFR fragment. Hence, preferential binding of part of this competing helix to either the target or library winner will not give rise to a colony under selective conditions and serves as a test of specificity under these competing conditions. Cells expressing either a six-residue mock sequence (pAR410d-mock) or the Fos homologue cFos—FosB−Fra1—Fra2 fusion competing peptide on this plasmid (pAR410d-cFos-FosB-Fra1-Fra2-eGFP) were grown in M9 minimal medium (100 μg/mL Amp, 25 μg/mL *Cm*, 50 μg/mL Kan, 25 μg/mL Tet, 1 μg/mL trimethoprim, and 1 mM IPTG) by inoculating an M9 solution from a midlog preculture to a starting OD_{600} of 0.01 under selective conditions.

Peptide Synthesis and Purification. Peptides were synthesized by Protein Peptide Research (PPR Ltd., Fareham, U.K.) and subsequently purified to >98% purity using RP-HPLC with

Table 1: Peptide Sequences

cJun	ASIARLEEKVKTLKAQNYELASTANMLREQVAQLGAP
cFos	ASTDTLQAETDQLEDEKYALQTEIANLLKEKEKLGAP
FosB	ASTDRLQAETDQLEEEKYELESEIAELQKEKERLGAP
Fra1	ASTDFLQAETDKLEDEKYGLQREIEELQKQKERLGAP
Fra2	ASTEKLQAETEELEEEKYGLQKEIAELQKEKEKLGAP
FosW	ASLDELQAEIEQLEERNYALRKEIEDLQKQLEKLGAP
$FosW_{e/g}$	ASLDELQAEIEQLGEGNYALRKEIEDLKKQLEKLGAP
$FosW_{Core}$	ASIDELQAEVEQLEERNYALRKEVEDLQKQAEKLGAP

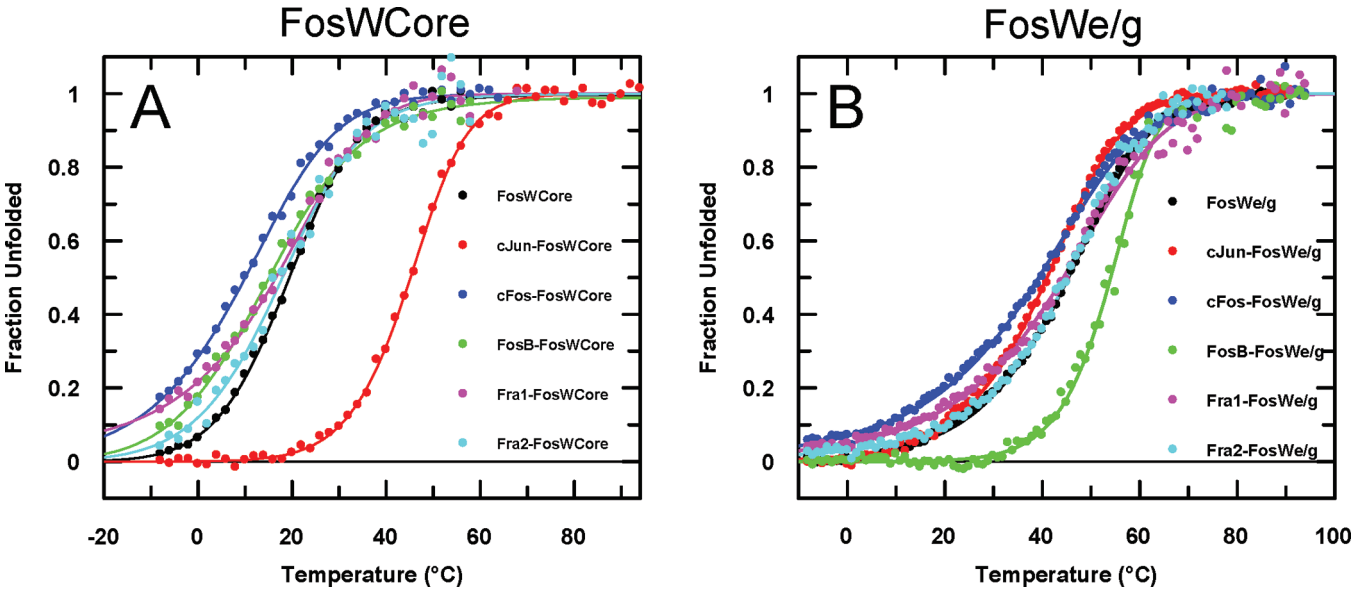

FIGURE 2: Thermal stability of peptide pairs measured using the temperature dependence of the CD signal at 222 nm. Data are shown for (A) $FosW_{Core}$ and (B) $FosW_{e/g}$ peptides paired with the PCA target cJun (desired state, colored red), as well as the individual component sequences of the Fos homologue fusion peptide competitor sequence (i.e., cFos colored blue, FosB colored green, Fra1 colored magenta, and Fra2 colored cyan). Homodimeric data for the two winners are colored black. Lines represent fits to the data according to a two-state model (eq 1). Thermal melting (T_m) values derived from these fits are listed in Table 2. Data were fitted using Grafit (Erithacus Software Ltd.).

a Jupiter Proteo column [4 μm particle size, 90 Å pore size, 250 mm × 10 mm (Phenomenex)] and a gradient from 5 to 50% acetonitrile (0.1% TFA) over 50 min at a rate of 1.5 mL/min. Correct masses were verified by electrospray mass spectrometry. The peptides in Table 1 were synthesized as amidated and acetylated peptides and contained N- and C-capping motifs (underlined) for improved helix stability and solubility. Peptide concentrations were determined in water using the absorbance at 280 nm with an extinction coefficient of 1209 M^{-1} cm^{-1} (*21*) corresponding to a Tyr residue inserted into a solvent-exposed **b3** heptad position.

Circular Dichroism Measurements. Spectra and thermal melts were performed at a total peptide concentration of 150 μM in 10 mM potassium phosphate and 100 mM potassium fluoride (pH 7) using a Jasco J-810 CD instrument. The temperature was ramped at a rate of 0.5 °C/min. Melting profiles (see Figure 2) were ≥94% reversible. Equilibrium denaturation curves were fitted to a two-state model to yield the melting temperature (T_m, the temperature at which the protein is 50% unfolded):

$$\Delta G = \Delta H - (T_A/T_m)[\Delta H + RT_m \times \ln(P_t)] + \Delta C_p[T_A - T_m - T_A \times \ln(T_A/T_m)] \quad (1)$$

where ΔH is the change in enthalpy, T_A is the reference temperature, R is the ideal gas constant (1.9872 cal mol^{-1} K^{-1}), P_t is the total peptide concentration (150 μM), and ΔC_p is the change in heat capacity (see also ref *24*). T_m values were determined by least-squares fitting of the denaturation curves (see Figure 2 and Table 2) assuming a two-state folding model that is widely used for coiled coils and provided an excellent fit to our data. Melting profiles for heterodimers are clearly distinct from averages of constituent homodimeric melts, indicating that helices are dimerizing in an apparent two-state process that is consistent with a dimeric protein. The T_m values were found to be accurate within 1 °C for the same dimer studied several months apart and from a different sample (unpublished data). Data collection for all temperature denaturation experiments was started at −8 °C, and at this temperature, the peptide solutions remained aqueous, even when left overnight. Data points for thermal denaturation profiles represent the averaged signal after data collection for 4 s. Protein folding studies have demonstrated that for GCN4, a yeast homologue of AP-1, both binding and dissociation of dimers are tightly coupled with folding and unfolding of the individual helices, and are described well by a simple

Table 2: Thermal Unfolding Data, K_D Values, and bCIPA Predictions

		$FosW_{Core}$	$FosW_{e/g}$
cJun	T_m (°C)[a]	45 ± 0.1	41 ± 0.1
	$K_{D,37\ °C}$[b]	20 μM	72 μM
	prediction 1[c]	62	58
	prediction 2[d]	35	38
cFos	T_m (°C)[a]	10 ± 0.2	39 ± 0.2
	$K_{D,37\ °C}$[b]	6.8 mM	109 μM
	prediction 1[c]	10	28
	prediction 2[d]	6	23
FosB	T_m (°C)[a]	15 ± 0.2	54 ± 0.2
	$K_{D,37\ °C}$[b]	3.7 mM	1.7 μM
	prediction 1[c]	26	49
	prediction 2[d]	7	25
Fra1	T_m (°C)[a]	17 ± 0.3	44 ± 0.3
	$K_{D,37\ °C}$[b]	2.9 mM	47 μM
	prediction 1[c]	14	37
	prediction 2[d]	1	20
Fra2	T_m (°C)[a]	18 ± 0.4	45 ± 0.1
	$K_{D,37\ °C}$[b]	3.5 mM	37 μM
	prediction 1[c]	29	51
	prediction 2[d]	3	21
homodimer	T_m (°C)[a]	19 ± 0.1	45 ± 0.1
	$K_{D,37\ °C}$[b]	3.8 mM	34 μM
	prediction 1[c]	47	104
	prediction 2[d]	−1	37

[a]Thermal unfolding value taken from circular dichroism studies using eq 1 (Figure 2). [b]Corresponding $K_{D,37\ °C}$ values were estimated from a plot of ln K_D vs temperature using fraction unfolded (f_u) data from the transition region. [c]Predicted thermal melting values based on the bZIP coiled coil interaction prediction algorithm (bCIPA) (*17*). [d]Base-optimized weight scoring taken from the bZIP Coiled Coil Scoring Form (*33*).

Table 3: Energetic Contributions of Core **a**−**a′** Coupling Energies

	a1−**a1′**		**a2**−**a2′**		**a3**−**a3′**		**a4**−**a4′**		**a5**−**a5′**		total
ΔΔ*G* (FosW$_{Core}$/cJun)[a]	**II**	**−9.2**[b]	**VV**	**−5.4**	**NN**	**−2.4**	**VA**	**−2.4**	**AV**	**−2.4**	**−21.8**
ΔΔ*G* (FosW$_{Core}$/Fos)	IT	−1.5	VT	−1.3	NK	−0.1	VI	−6.2	AK	1.3	−7.8
ΔΔΔ*G* (*FosW$_{Core}$*/*cJun* − *FosW$_{Core}$*/*Fos*)[c]		*−7.7*[d]		*−4.1*		*−2.3*		*3.8*		*−3.7*	*−14.0*
ΔΔ*G* (FosW$_{Core}$/FosW$_{Core}$)	II	−9.2	VV	−5.4	NN	−2.4	VV	−5.4	AA	0	−22.4
ΔΔΔ*G* (*FosW$_{Core}$*/*cJun* − *FosW$_{Core}$*/*FosW$_{Core}$*)		*0.0*		*0.0*		*0.0*		*3.0*		*−2.4*	*0.6*
ΔΔ*G* (FosW$_{e/g}$/cJun)[e]	**LI**	**−5.8**	**IV**	**−6.2**	**NN**	**−2.4**	**IA**	**−4.2**	**LV**	**−4.5**	**−23.1**
ΔΔ*G* (FosW$_{e/g}$/Fos)	LT	−0.9	IT	−1.5	NK	−0.1	II	−9.2	LK	−1.2	−12.9
ΔΔΔ*G* (*FosW$_{e/g}$*/*cJun* − *FosW$_{e/g}$*/*Fos*)		*−4.9*		*−4.7*		*−2.3*		*5.0*		*−3.3*	*−10.2*
ΔΔ*G* (FosW$_{e/g}$/FosW$_{e/g}$)	**LL**	**−5.2**	**II**	**−9.2**	**NN**	**−2.4**	**II**	**−9.2**	**LL**	**−5.2**	−31.2
ΔΔΔ*G* (*FosW$_{e/g}$*/*cJun* − *FosW$_{e/g}$*/*FosW$_{e/g}$*)		*−0.6*		*3.0*		*0.0*		*5.0*		*0.7*	*8.1*
difference (FosW$_{Core}$ − FosW$_{e/g}$) (desired − undesired heterodimer)		−2.8[f]		0.6		0.0		−1.2[f]		−0.4	−3.8
difference (FosW$_{Core}$ − FosW$_{e/g}$) (desired − undesired homodimer)		0.6		−3.0		0.0		−2.0		−3.1	−7.5

[a]Boldface indicates the desired heterodimeric FosW$_{Core}$−cJun or FosW$_{e/g}$−cJun interaction. [b]Values are given in kilocalories per mole and were taken from ref *30*. [c]Italics indicate the difference between the desired interaction and the indicated competing interaction, i.e., either interaction with Fos or homodimerization. [d]Underlined values emphasize more stable interactions for the desired state compared to the competing state. [e]Energetic contributions for many **e**/**g** coupling energies are not known (GA/GQ/GE/EL/EQ/QT/KT), and therefore, no estimation of the overall contribution to stability for electrostatics could be established. [f]Note that the bulk of the specificity of FosW$_{Core}$ for cJun relative to FosW$_{e/g}$ for cJun comes from the I-I pair at the **a1** and **a1′** positions in the desired state for the former (−2.8 kcal/mol) and the I-I pair introduced at the **a4** and **a4′** positions in the nondesired state for the latter (−1.2 kcal/mol).

two-state model (*22*, *23*). Our own studies have shown, at least for cFos−JunW-based peptides, that folding occurs via an intermediate that is undetectable in equilibrium denaturation experiments (*24*).

RESULTS

We previously screened a library based on cJun to derive a peptide (JunW$_{CANDI}$) capable of binding specifically and with high affinity to cFos in the presence of a cJun competitor. In contrast, selection of a cFos-based library designed to yield a high-affinity binder for cJun in the presence of a cFos did not yield the desired specificity. This was caused by the fact that the eight randomized positions were collectively unable to generate a peptide that could target cJun specifically in the presence of cFos (*25*). Nonetheless, cJun is a valuable target; sequestering cJun will release the Fos homologues which are known to be unable to homodimerize and are therefore unlikely to give rise to an oncogenic phenotype (*26*). The tested library offered a small set of residue options at core **a** positions (four of five positions with L, I, and V, all combinations which result in a high interaction stability with cJun) and **e**/**g** positions [four of eight positions with **g2** (E, Q, R), **g4** (E, Q), **e3** (Q, R), and **e4** (L, Q, R)] and ultimately failed because the peptide library lacked the electrostatic and core options able to collectively impose specificity upon the library winner (*25*). Continuing from these findings, we investigate whether modification of either the **a** or **e**/**g** residues alone would be sufficient to confer specificity upon the interaction with the target solely based on positive design.

FosW$_{Core}$ Randomization. The core **a** library contained 12 residue options (codon NHT = F, L, I, V, S, P, T, A, Y, H, N, or D) at four of five **a** position residues. The central Asn residue **a3**, which pairs with Asn$_{a3'}$ in the desired state, was not changed as this Asn-Asn pairing is key in maintaining the dimeric specificity, orientation, and dimer heptad alignment (*27*−*29*) and contributes −2.4 kcal/mol of pairing energy for the desired Fos−Jun species (*30*). Since Fos contains Lys at **a3**, the Asn-Lys pair for nondesired complexes is unfavorable (0.1 kcal/mol). The residue pairings are, however, identical for FosW and FosW$_{e/g}$ (see Figure 1). Likewise, the electrostatic **e**/**g** residues of FosW$_{Core}$ as well as all outer residues (**b**, **c**, and **f** positions) were identical to those of FosW.

All four residues were selected by the third passage in liquid growth PCA competitions. Reassuringly, it is noteworthy that from the 12 possible residue options, only I, V, and A were selected, all of which are of high helical propensity, individually make significantly different contributions to overall dimer stability (see Figure 1), and are the most abundant residues in both natural and designed dimeric coiled coil interfaces (*30*). The overall residue changes of FosW$_{core}$ relative to FosW were therefore as follows: **a1** Leu → Ile, **a2** Ile → Val, **a4** Ile → Val, and **a5** Leu → Ala.

In the characterization of the stability as a heterodimer with individual peptides from the competing fusion helix, the PCA-selected FosW$_{Core}$ was found to bind to its target cJun with the highest stability (T_m = 45 °C) and to all of the competitors with significantly lower stability [T_m = 10, 15, 17, and 18 °C for complexes with cFos, FosB, Fra1, and Fra2, respectively (Table 2 and Figure 2)]. In addition, FosW$_{Core}$ homodimerized with a T_m of only 19 °C in stark contrast to FosW (homodimeric T_m = 57 °C), where core options were limited to three residues (L, I, and V).

The difference between desired heterodimer and nondesired homodimer stabilities for FosW$_{Core}$ versus FosW **a** residues is most likely due to the loss of one Ile-Ile pair (**a4**), and the introduction of an Ala-Ala pair (**a5**) in FosW$_{Core}$, resulting in a loss of ∼8.8 kcal/mol according to published energy differences (*27*, *28*) (Figure 1). The Ile-Ile core residue pair buries a significant amount of hydrophobic material and makes a large contribution to the free energy of folding [e.g., $\Delta\Delta G_{AA\rightarrow II}$ = −9.2 kcal/mol (*27*, *28*)]. In this respect, a slight decrease in the stability of the desired state (Ile-Ala for FosW−cJun and Val-Ala for FosW$_{Core}$−cJun at **a4**−**a4′**) is outweighed by the larger energy difference in the nondesired homodimer ($\Delta\Delta\Delta G_{IA\rightarrow VA}$ = 1.8 kcal/mol vs $\Delta\Delta\Delta G_{II\rightarrow VV}$ = 3.8 kcal/mol) (Table 3). Therefore, FosW$_{Core}$ binds to Fos homologues with low stability, whereas FosW binds Fos homologues with rather higher stability [T_m values of 10−19 °C for the former and 52−61 °C for the latter (see Table 2)]. This is possibly also due to the removal of an Ile-Ile **a4**−**a4** pair.

The selection of Ala at position **a5** of $FosW_{core}$ appears to be important, as this contributes favorably in the desired complex paring with $V_{a5'}$ ($\Delta\Delta G_{AV} = -2.4$ kcal/mol) relative to Ala-Ala pairs in the homodimer ($\Delta\Delta\Delta G_{AV\rightarrow AA} = 2.4$ kcal/mol). In contrast, in FosW, leucine at **a5** gives L-V (−4.5 kcal/mol) for the desired and L-L (−5.2 kcal/mol) for the nondesired homodimer and, thus, similar energetic differences between desired and nondesired states ($\Delta\Delta\Delta G_{LV\rightarrow LL} = -0.7$ kcal/mol) (Table 3). Although the Jun and Fos cores are distinct, cores for all Fos homologues are the same. In essence, therefore, the $FosW_{Core}$ library needs only to make two distinctions. In contrast, **e**/**g** residues are slightly different for every Fos homologue as well as in the desired cJun target (see Figure 1 and Table 3).

Summing the overall energetic contributions (Table 3) reveals that the gain of one Ile-Ile pair (for $FosW_{Core}$−cJun **a1**−**a1′**) and the loss of a different Ile-Ile pair (for $FosW_{Core}$−Fos **a4**−**a4′**) are responsible for the bulk of the favorable free energy for the $FosW_{Core}$−cJun pair relative to other dimeric pairs. Explicitly, the **a1**−**a1′** Ile-Ile pair of $FosW_{Core}$−cJun is replaced by an Ile-Thr pair for $FosW_{Core}$−Fos-based dimers, representing a favorable energy difference of 7.7 kcal/mol for the desired species (compared to an energy difference of only 4.9 kcal/mol in the case of FosW−cJun vs FosW−Fos). In contrast, whereas FosW−cJun contains a favorable Ile-Ala pair, in FosW−Fos dimers the **a4** and **a4′** positions are occupied by an Ile-Ile pair, representing a −5.0 kcal/mol energetic contribution toward these nondesired complexes. Consequently, large energetic gains are a result of these Ile-Ile changes, for the **a1**−**a1′** Ile-Ile pairs ($FosW_{Core}$−cJun) in the desired state, and via removal of stabilizing Ile-Ile **a4**−**a4′** pairs (FosW−Fos) in the nondesired state (see Table 3).

These results imply that a negative design strategy may not be implicitly required in the design process because of a large number of options available in the library that result in a large energetic contributory range accessible to the core. The core may already be close or at the optimum and thus exert enough stability on the desired interaction for specificity to be generated without being implicitly required by a negative design strategy (*20*, *29*, *30*). Using this information at the start of the design process could significantly simplify the overall approach.

$FosW_{e/g}$ Randomization. In a second library, all six electrostatic **e**/**g** residues that make specific contacts in the target helix were randomized. Both positively and negatively charged as well as polar residues were introduced into this **e**/**g** library (codon VRG = Gln, Lys, Arg, Glu, and Gly). The overall changes for $FosW_{e/g}$ relative to the FosW template were as follows: **g2** Arg → Gly, **e2** Glu → Gly, and **e4** Gln → Lys. $FosW_{e/g}$ was found to bind cJun with a T_m of 41 °C. However, it did so with all of the competing states, with T_m values of 39 °C (with cFos), 54 °C (with FosB), 44 °C (with Fra1), 45 °C (with Fra2), and 45 °C (as a homodimer) (Figure 2 and Table 2). One surprising finding was that the selection of Gly at positions **e2** and **g2** did not compromise the stability of the helix enough to significantly impair the dimeric T_m values. The introduction of a glycine residue option was originally intended to serve as a negative control and was not predicted to have been selected. Rather, as a consequence of the increased Ramachandran space accessible for a glycine side chain (*31*), its inclusion in $FosW_{e/g}$ was expected to have led to an overall loss of helical stability, although a T_m of 41 °C for $FosW_{e/g}$−cJun suggested that this was not as pronounced as might have been expected. Indeed, Agadir (*32*, *33*) predicts $FosW_{e/g}$ to have a higher helical content than $FosW_{Core}$,

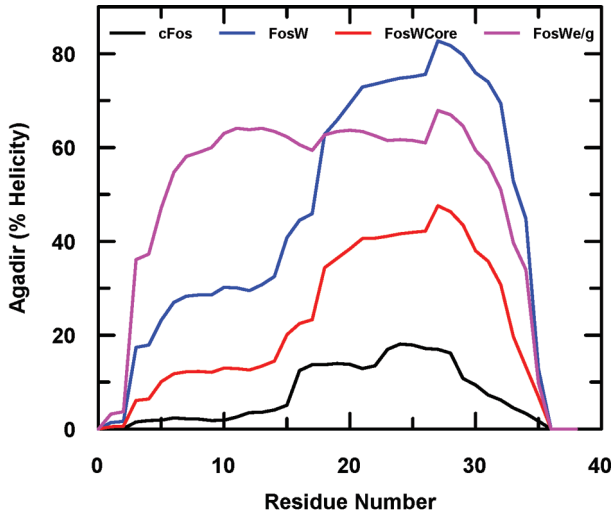


```
cFos       ASTDTLQAETDQLEDEKYALQTEIANLLKEKEKLGAP
FosW       ASLDELQAEIEQLEERNYALRKEIEDLQKQLEKLGAP
FosWCore   ASIDELQAEVEQLEERNYALRKEVEDLQKQAEKLGAP
FosWe/g    ASLDELQAEIEQLGEGNYALRKEIEDLKKQLEKLGAP
```

FIGURE 3: Helical content prediction at the residue level as calculated by AGADIR (*32*, *33*). The increased helicity of Fos-based PCA selected winner peptides is shown relative to that of cFos. cFos (black line) has the lowest helical propensity (< 20%) throughout the sequence. FosW (blue) has improved helical propensity, particularly at the C-terminus, whereas $FosW_{e/g}$ (magenta) has a higher predicted helicity than FosW toward the N-terminus but also maintains a relatively high helicity at the C-terminus. In contrast, $FosW_{Core}$ (red) has a lower predicted helicity than FosW or $FosW_{e/g}$, but an improved helicity relative to that of the cFos parent sequence. These predictions agree well with absolute helical signals at 222 nm taken from thermal melts, where at 37 °C $\theta_{222} = -13000, -17914, -5062$, and −3914 for FosW, $FosW_{e/g}$, $FosW_{Core}$, and cFos, respectively. Shown below are the sequences corresponding to the above residue number.

a higher helical content than FosW at its N-terminus, and an only marginally lower helical content than FosW at the C-terminus (Figure 3). Another general hypothesis for why strong energetic discrimination was not possible in this system comes from the lower energetic contribution to stability from **e**/**g** pairs; the greatest measured contribution relative to an AA pair (i.e., $\Delta\Delta G$) is −1.45 kcal/mol for an E-R pair, in comparison to a $\Delta\Delta G$ of −9.2 kcal/mol for an I-I pair in the core. This means > 6-fold more stability is offered by an optimal core pairing than an optimal **e**/**g** pairing, relative to an A-A pair at the respective positions. This suggests that gaining specificity (negative design) as a consequence of positive design is perhaps too demanding a task for this selection. Hydrophobic core residues additionally make their contribution early in the folding pathway, favoring the folded state by lowering the energetic barrier to folding (*24*). In addition, the five core **a** residues for competing states are the same (T, T, K, I, and K for **a1**, **a2**, **a3**, **a4**, and **a5**, respectively), meaning that only one residue change is required to create significant energetic differences between the desired state and nondesired states. In contrast, the **e**/**g** residues of competing states differ from each other as well as the target.

Growth Competitions. In addition to thermal denaturation studies, the influence of competing states was assessed using bacterial growth competitions. This involved transformation of *E. coli* BL21 containing a target peptide (cJun) together with the PCA selection winner peptide (either $FosW_{Core}$ or $FosW_{e/g}$), both as DHFR fragment fusions. Cells contained another plasmid conferring tetracycline resistance and expressing either a Fos

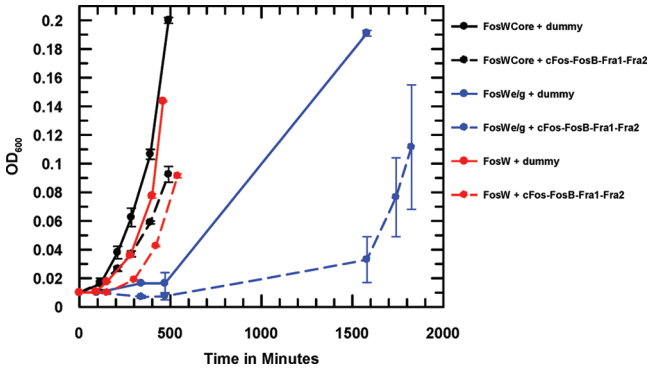

FIGURE 4: Bacterial growth rates for *E. coli* BL21 cells expressing cJun−DHFR1 (Amp^R), pREP4 (Kan^R) for lac repression, and either $FosW_{Core}$ or $FosW_{e/g}$ (Cm^R). A fourth plasmid (tet^R) expressed either a short six-amino acid mock peptide or the Fos homologue fusion peptide competitor (cFos−FosB−Fra1−Fra2−eGFP). The mock sequence was included as a control for reduced bacterial growth rates due to additional antibiotic stress. M9 starter cultures were created in duplicate and grown to midlog phase, before assay growths were initiated at an OD_{600} of 0.01. The growth rate of cells expressing $FosW_{Core}$ was only slightly retarded for cells expressing the Fos homologue fusion peptide competitor (black dashed line) relative to the mock peptide (black solid line). In contrast, cells expressing $FosW_{e/g}$ and the mock sequence (blue solid line) grew much slower, and expression of the Fos homologue fusion peptide competitor (blue dashed line) retarded this growth rate considerably further. Also shown is the original FosW sequence with mock peptide (red solid line) and with fusion competitor peptide (red dashed line).

homologue fusion peptide competitor or a six-residue mock sequence as a control. The Fos homologue fusion peptide competitor consisted of a $(His)_6$ tag−cFos−FosB−Fra1−Fra2−eGFP fusion protein (each helix is separated by Gly-Ala-Pro-Ala-Ser linkers designed to disrupt helicity and to add flexibility between helices). The competing sequence was created as a fusion protein for simplification of the system (rather than expressing four proteins separately) and was expressed on a third plasmid in the absence of a DHFR fragment fusion (*25*). It should be noted that all possible pairings of cFos, FosB, Fra1, and Fra2 have been previously characterized (*17*, *18*) and are known to be particularly unstable (all T_m values range from −19 to 1 °C, with the exception of homodimeric Fra2, which displays a T_m of 19 °C), and therefore, the Fos homologue fusion peptide competitor is not predicted to self-associate in the cell. In addition, using an Ni-NTA column, we were able to purify several milligrams of the green fusion protein from just 1 L of bacterial culture, indicating that the fusion peptide is well expressed and not susceptible to significant amounts of proteolytic degradation.

Under selective conditions, *E. coli* growth rates for PCA winning cells were monitored when they were additionally transformed with either the cFos−FosB−Fra1−Fra2 fusion or the mock sequence, and the growth rates of the cells were compared. In this scenario, the reduction in growth rate caused purely by the loss in specificity of the winner for cJun could be determined (see Figure 4).

Since $FosW_{e/g}$ has a high homodimeric stability (45 °C) relative to that of $FosW_{Core}$ (19 °C), growth competitions conducted under selective conditions in the presence of a mock helix revealed that cells expressing cJun−DHFR1 and $FosW_{e/g}$−DHFR2 took in excess of 11 h to reach an OD_{600} of 0.05 (from 0.01) compared to less than 4 h for $FosW_{Core}$−DHFR2 (see Figure 4). This effect is enhanced when the cFos−FosB−Fra1−Fra2 competing helix is expressed instead of the mock peptide: Cells expressing $FosW_{Core}$ reached an OD_{600} of 0.05 in just <6 h, whereas cells expressing $FosW_{e/g}$ took some 27 h. This is in close agreement with the thermal melting data (Figure 2 and Table 2) that demonstrate $FosW_{e/g}$ forms a stable dimer with all nondesired species (dimer stabilities range from 39 to 54 °C, compared to 41 °C for the desired interaction), whereas $FosW_{Core}$ does not (dimer stabilities range from 10 to 19 °C, compared to 45 °C for the desired interaction). Lastly, as a control, cells expressing the previously selected FosW (*17*) grew at a rate comparable to that of $FosW_{Core}$ despite distinctly different thermal melting values with cJun (63 °C for cJun−FosW vs 45 °C for cJun−$FosW_{Core}$), suggesting that this excess of stability of FosW is partially compromised by the higher stability of the nondesired complexes (T_m = 61, 52, 54, 56, and 57 °C for complexes with cFos, FosB, Fra1, Fra2, and the FosW homodimer, respectively).

It is also notable that the difference in growth rates for cells expressing FosW, cJun, and the cFos−FosB−Fra1−Fra2 fusion protein relative to those expressing a mock helix did not vary significantly from that of $FosW_{Core}$ cells expressing fusion helix relative to the mock sequence (Figure 4). This is likely to be due to the fact that for FosW the desired state is very stable and favored over the nondesired states, albeit with a difference of only 2 °C for the most stable nondesired state. $FosW_{Core}$ is specific with or without expression of the fusion helix, and therefore, no large reduction in growth rate is observed. In stark contrast, the growth rate of cells expressing $FosW_{e/g}$ and the Fos homologue fusion peptide competitor was significantly reduced relative to that of the mock sequence. This effect can be explained by the similarity in energies of desired and nondesired states with four nondesired complexes displaying slightly higher stability than the desired state.

DISCUSSION

We have demonstrated the ability of PCA to generate a peptide ($FosW_{Core}$) that is both stable and specific for cJun. This peptide was based on a previously selected FosW template (*17*). Importantly, it was generated from a library with more options than those open to the FosW selection, but in which only core residues (**a1**, **a2**, **a4**, and **a5**) were randomized, generating 12 residue options for each position. The resulting $FosW_{Core}$−cJun dimer displayed a T_m of 45 °C and a ΔT_m of 26 °C with respect to the next most stable competing interaction ($FosW_{Core}$ homodimer). Indeed, although residues selected at positions **a1**, **a2**, and **a4** were contained within the first library, Ala selected at position **a5** was not. As described previously, this Ala was very important in reducing the stability of the homodimer, i.e., negative design. Consequently, for the assay, the larger energy difference between the desired and nondesired pair seems to be more important than the higher stability of the first FosW. This is seen in the growth experiments with the mock peptide.

In contrast, a FosW-based library that was randomized to produce five options at all six contacting electrostatic positions did not yield a peptide ($FosW_{e/g}$) capable of conferring specificity for cJun.

Additionally, the PCA selection is likely to reach an optimum and go into saturation if enough active enzyme is made, with variation in expression levels also possibly influencing assay performance (*32*). Indeed, both $FosW_{Core}$ and $FosW_{e/g}$ sequences, despite being less stable than their parent FosW peptide, bound to cJun with high stability [$FosW_{Core}$−cJun T_m = 45 °C, $FosW_{e/g}$−cJun T_m = 41 °C, and FosW−cJun T_m = 63 °C

(Figure 2)]. The effect of large FosW-based libraries, semirandomized at either core or electrostatic positions, on the stability and specificity of binding with cJun produced three observations.

(i) Because of the larger energetic range of contributions that are permissible, the core residues are able to generate much larger energetic gaps between desired and nondesired complexes and with fewer residue changes, making possible negative design as a byproduct of positive design. (ii) Fos cores are the same for all four homologues, whereas the **e**/**g** residues are distinct for each, making negative design more achievable for the core library relative to the **e**/**g** library. As a consequence of observations (i) and (ii), (iii) there must be many preferential **e**/**g** changes for the desired interaction if specificity is to be achieved via electrostatic-based libraries alone.

It should also be noted that, as is the case with cFos−cJun, when all proteins are present in solution, the lower the stability of the homodimeric winner, the more the equilibrium is shifted in the direction of the more stable (desired) species. This scenario would favor a stable and specific interaction of the antagonist with its target, as is the case for $FosW_{Core}$. This is verified by growth competitions, which show that $FosW_{Core}$−cJun confers faster growth than $FosW_{e/g}$−cJun because of the relative instability of homodimeric $FosW_{Core}$. This is exacerbated by expression of the cFos−FosB−Fra1−Fra2 competitor peptide which, in agreement with thermal melting data, binds $FosW_{e/g}$ with higher affinity than even the desired complex (T_m values range from 39 to 54 °C with two of these exceeding the T_m of the desired state by 9 °C) than $FosW_{Core}$ (T_m values of 10−19 °C).

Since we are now able to achieve reasonable stabilities for the desired state, with K_D values in the low micromolar range (see Table 2), our next aim is to reduce the size of peptide libraries that are being screened. This large-scale task will require a significant amount of time to undertake and will use the findings of this study as a basis for initial designs. In particular, shortened peptides will serve a 2-fold purpose. (i) Peptides are moved toward the range of more druggable peptidomimetic-based molecules. (ii) Using smaller peptides, a proportionally larger range of residues can be randomized in the screening process. It should be noted that despite this task being beyond the scope of this initial study, we anticipate that $FosW_{Core}$ in particular will form an excellent starting point for further optimization involving semirandomized residues at core and electrostatic positions. Subsequently, a greater relative proportion of the overall molecule can be randomized in future reduced length peptides for efficient screening of residue options.

ACKNOWLEDGMENT

We thank Kristian M. Müller for critical reading of the manuscript. We also thank Karin Schmidtkunz for excellent technical assistance throughout this work.

REFERENCES

1. Shaulian, E., and Karin, M. (2002) AP-1 as a regulator of cell life and death. *Nat. Cell Biol. 4*, E131–E136.
2. Eferl, R., and Wagner, E. F. (2003) AP-1: A double-edged sword in tumorigenesis. *Nat. Rev. Cancer 3*, 859–868.
3. Hess, J., Angel, P., and Schorpp-Kistner, M. (2004) AP-1 subunits: Quarrel and harmony among siblings. *J. Cell Sci. 117*, 5965–5973.
4. Mason, J. M., and Arndt, K. M. (2004) Coiled coil domains: Stability, specificity, and biological implications. *ChemBioChem 5*, 170–176.
5. Mason, J. M., Muller, K. M., and Arndt, K. M. (2007) Considerations in the design and optimization of coiled coil structures. *Methods Mol. Biol.* (*Totowa, NJ, U.S.*) *352*, 35–70.
6. Glover, J. N., and Harrison, S. C. (1995) Crystal structure of the heterodimeric bZIP transcription factor c-Fos-c-Jun bound to DNA. *Nature 373*, 257–261.
7. Xu, Y., Zhu, J., Liu, Y., Lou, Z., Yuan, F., Liu, Y., Cole, D. K., Ni, L., Su, N., Qin, L., Li, X., Bai, Z., Bell, J. I., Pang, H., Tien, P., Gao, G. F., and Rao, Z. (2004) Characterization of the heptad repeat regions, HR1 and HR2, and design of a fusion core structure model of the spike protein from severe acute respiratory syndrome (SARS) coronavirus. *Biochemistry 43*, 14064–14071.
8. Bianchi, E., Finotto, M., Ingallinella, P., Hrin, R., Carella, A. V., Hou, X. S., Schleif, W. A., Miller, M. D., Geleziunas, R., and Pessi, A. (2005) Covalent stabilization of coiled coils of the HIV gp41 N region yields extremely potent and broad inhibitors of viral infection. *Proc. Natl. Acad. Sci. U.S.A. 102*, 12903–12908.
9. Brown, J. H., Cohen, C., and Parry, D. A. (1996) Heptad breaks in α-helical coiled coils: Stutters and stammers. *Proteins 26*, 134–145.
10. Sharma, V. A., Logan, J., King, D. S., White, R., and Alber, T. (1998) Sequence-based design of a peptide probe for the APC tumor suppressor protein. *Curr. Biol. 8*, 823–830.
11. Siegert, R., Leroux, M. R., Scheufler, C., Hartl, F. U., and Moarefi, I. (2000) Structure of the molecular chaperone prefoldin: Unique interaction of multiple coiled coil tentacles with unfolded proteins. *Cell 103*, 621–632.
12. Kitamura, K., Tanaka, H., and Nishimune, Y. (2005) The RING-finger protein haprin: Domains and function in the acrosome reaction. *Curr. Protein Pept. Sci. 6*, 567–574.
13. Borghouts, C., Kunz, C., and Groner, B. (2005) Current strategies for the development of peptide-based anti-cancer therapeutics. *J. Pept. Sci. 11*, 713–726.
14. Davis, J. M., Tsou, L. K., and Hamilton, A. D. (2007) Synthetic non-peptide mimetics of α-helices. *Chem. Soc. Rev. 36*, 326–334.
15. Pelletier, J. N., Campbell-Valois, F. X., and Michnick, S. W. (1998) Oligomerization domain-directed reassembly of active dihydrofolate reductase from rationally designed fragments. *Proc. Natl. Acad. Sci. U.S.A. 95*, 12141–12146.
16. Arndt, K. M., Pelletier, J. N., Müller, K. M., Alber, T., Michnick, S. W., and Plückthun, A. (2000) A heterodimeric coiled-coil peptide pair selected in vivo from a designed library-versus-library ensemble. *J. Mol. Biol. 295*, 627–639.
17. Mason, J. M., Schmitz, M. A., Müller, K. M., and Arndt, K. M. (2006) Semirational design of Jun-Fos coiled coils with increased affinity: Universal implications for leucine zipper prediction and design. *Proc. Natl. Acad. Sci. U.S.A. 103*, 8989–8994.
18. Mason, J. M., Mueller, K. M., and Arndt, K. M. (2008) iPEP: Peptides designed and selected for interfering with protein interaction and function. *Biochem. Soc. Trans. 36*, 1442–1447.
19. Bolon, D. N., Grant, R. A., Baker, T. A., and Sauer, R. T. (2005) Specificity versus stability in computational protein design. *Proc. Natl. Acad. Sci. U.S.A. 102*, 12724–12729.
20. Appleman, J. R., Prendergast, N., Delcamp, T. J., Freisheim, J. H., and Blakley, R. L. (1988) Kinetics of the formation and isomerization of methotrexate complexes of recombinant human dihydrofolate reductase. *J. Biol. Chem. 263*, 10304–10313.
21. Du, H., Fuh, R. A., Li, J., Corkan, A., and Lindsey, J. S. (1998) PhotochemCAD: A computer-aided design and research tool in photochemistry. *Photochem. Photobiol. 68*, 141–142.
22. Zitzewitz, J. A., Bilsel, O., Luo, J., Jones, B. E., and Matthews, C. R. (1995) Probing the folding mechanism of a leucine zipper peptide by stopped-flow circular dichroism spectroscopy. *Biochemistry 34*, 12812–12819.
23. Knappenberger, J. A., Smith, J. E., Thorpe, S. H., Zitzewitz, J. A., and Matthews, C. R. (2002) A buried polar residue in the hydrophobic interface of the coiled-coil peptide, GCN4-p1, plays a thermodynamic, not a kinetic role in folding. *J. Mol. Biol. 321*, 1–6.
24. Mason, J. M., Hagemann, U. B., and Arndt, K. M. (2007) Improved Stability of the Jun-Fos Activator Protein-1 Coiled Coil Motif: A Stopped-Flow Circular Dichroism Kinetic Analysis. *J. Biol. Chem. 282*, 23015–23024.
25. Mason, J. M., Mueller, K. M., and Arndt, K. M. (2007) Positive aspects of negative design: Simultaneous selection of specificity and interaction stability. *Biochemistry 46*, 4804–4814.
26. O'Shea, E. K., Rutkowski, R., and Kim, P. S. (1992) Mechanism of specificity in the Fos-Jun oncoprotein heterodimer. *Cell 68*, 699–708.
27. Lumb, K. J., and Kim, P. S. (1995) A buried polar interaction imparts structural uniqueness in a designed heterodimeric coiled coil. *Biochemistry 34*, 8642–8648.
28. Gonzalez, L., Jr., Woolfson, D. N., and Alber, T. (1996) Buried polar residues and structural specificity in the GCN4 leucine zipper. *Nat. Struct. Biol. 3*, 1011–1018.

29. Lai, J. R., Fisk, J. D., Weisblum, B., and Gellman, S. H. (2004) Hydrophobic core repacking in a coiled-coil dimer via phage display: Insights into plasticity and specificity at a protein-protein interface. *J. Am. Chem. Soc. 126*, 10514–10515.
30. Acharya, A., Rishi, V., and Vinson, C. (2006) Stability of 100 homo and heterotypic coiled-coil a-a′ pairs for ten amino acids (A, L, I, V, N, K, S, T, E, and R). *Biochemistry 45*, 11324–11332.
31. Ramachandran, G. N., Ramakrishnan, C., and Sasisekharan, V. (1963) Stereochemistry of polypeptide chain configurations. *J. Mol. Biol. 7*, 95–99.
32. Hagemann, U. B., Mason, J. M., Muller, K. M., and Arndt, K. M. (2008) Selectional and mutational scope of peptides sequestering the Jun-Fos coiled-coil domain. *J. Mol. Biol. 381*, 73–88.
33. Fong, J. H., Keating, A. E., and Singh, M. (2004) Predicting specificity in bZIP coiled-coil protein interactions. *Genome Biol. 5*, R11.